Noise-enhanced phase synchronization in time-delayed systems

D. V. Senthilkumar,[1] M. Manju Shrii,[1,2] and J. Kurths[1,2,3]
[1]*Potsdam Institute for Climate Impact Research, 14473 Potsdam, Germany*
[2]*Institute for Physics, Humboldt University, 12489 Berlin, Germany*
[3]*Institute for Complex Systems and Mathematical Biology, University of Aberdeen, United Kingdom*
(Received 18 November 2011; published 27 February 2012)

We investigate the phenomenon of noise-enhanced phase synchronization (PS) in coupled time-delay systems, which usually exhibit non-phase-coherent attractors with complex topological properties. As a delay system is essentially an infinite dimensional in nature with multiple characteristic time scales, it is interesting and crucial to understand the interplay of noise and the time scales in achieving PS. In unidirectionally coupled systems, the response system adjust all its time scales to that of the drive, whereas both subsystems adjust their rhythms to a single (main time scale of the uncoupled system) time scale in bidirectionally coupled systems. We find similar effects for both a common and an independent additive Gaussian noise.

DOI: 10.1103/PhysRevE.85.026218 PACS number(s): 05.45.Xt, 05.45.Pq, 05.45.Jn

I. INTRODUCTION

Synchronization of interacting dynamical systems is an evergreen research topic receiving a flurry of attention because of its fundamental importance in understanding numerous natural phenomena [1–3]. Recent investigations in this line of research are focusing on dynamical systems with intrinsic delay and delay couplings [4–7] due to a rich variety of dynamical behaviors induced by delay [8]. Among different kinds of synchronization, phase synchronization (PS) plays a crucial role in understanding the large class of weekly interacting dynamical systems [1–3]. For instance, PS forms the basic mechanism of large-scale integration of the neural process in neural assemblies of the brain [9]. Recently, it has also been shown that PS links the working memory and long-term memory by facilitating neural communication and by promoting neural plasticity [10]. Further, the key role of coupling, delay, and noise in understanding the "resting state" of the human brain associated with daydreaming, inner rehearsal, etc., have been reported [11].

Effects of noise on synchronization have also been studied extensively [1–3]. The phenomenon of "bubbling," i.e., noise-induced desynchronization due to local instability of the synchronization manifold [12], is an example of a nonconstructive effect of noise. Nevertheless, noise can also induce and enhance synchronization in coupled and uncoupled oscillators [13]. The influence of stochastic forces is also of great importance in various applications [14]. For instance, the stochastic process in the central nervous system is essential for the expression of spatiotemporal patterns [11]. It has been shown that the neural connections are of variable loops such that the propagation of a signal through the loops can result in a large time-delay (synaptic delay), and it is also reported that the axons can generate a time-delay up to 300 ms [15]. As a consequence, the neural networks have intrinsic delay in their dynamics. Hence investigating noise effects on PS of delay dynamical systems will provide a better understanding on the stochastic process mediating the information processing in neurons.

Here, we will investigate the phenomenon of noise-enhanced PS in coupled time-delay systems along with its mechanism. Delay dynamical systems are essentially infinite dimensional in nature exhibiting highly non-phase-coherent chaotic or hyperchaotic attractors. In contrast to low-dimensional dynamical systems described by ordinary differential equations as studied in Ref. [13], time-delayed systems exhibit strongly pronounced multiple characteristic time scales [4]. As PS is the coincidence of characteristic time scales of interacting dynamical systems, it is crucial and interesting to understand the interplay of noise and the multiple time scales in achieving PS in such systems for various applications. Indeed, only a very few studies have been reported on PS in coupled time-delay systems [6,7], despite the difficulty in estimation of the phase explicitly in such systems. Recently, we have demonstrated PS experimentally using electronic circuits in a piecewise linear time-delay system with a threshold nonlinearity [6]. In particular, we will consider the same system with parameter mismatches and demonstrate that both an independent and a common additive noise can enhance PS. Interestingly, multiple time scales of a time-delay system are clearly identified from the return times of the flow to a Poincaré section. We find noise-enhanced PS in both basic coupling configurations: unidirectional and bidirectional. On the one hand the response system adjusts its time scales to that of the drive in achieving PS in a unidirectional coupling configuration. On the other hand, both subsystems adjust their rhythms to the main time scale of the uncoupled system to achieve PS in bidirectionally coupled systems. Further, we will show that phase slips are accompanied by small and large return times, which are not present in the noise-free system, due to the unlocked unstable periodic orbits present in the coupled system.

The plan of the paper is as follows: In Sec. II, we introduce the coupled piecewise linear time-delay system. We will demonstrate the phenomenon of noise-enhanced phase synchronization in unidirectionally coupled time-delay systems in Sec. III and in bidirectionally coupled time-delay systems in Sec. IV. Finally, we present our summary and conclusion in Sec. V.

II. COUPLED TIME-DELAY SYSTEM

We consider the following coupled piecewise linear time-delay system

$$\dot{x} = \omega_x[-x(t) + bf(x(t-\tau))] + \varepsilon_x[y(t) - x(t)] + \sigma\xi_x(t),$$
$$\dot{y} = \omega_y[-y(t) + bf(y(t-\tau))] + \varepsilon_y[x(t) - y(t)] + \sigma\xi_y(t), \quad (1)$$

where $\omega_x = 1.0$ and $\omega_y = 1.1$ contributes to the frequency mismatch, $b = 1.2$ is the nonlinear parameter, $\tau = 1.33$ is the delay, $\varepsilon_{x,y}$ is the coupling strength, $\xi_{x,y}(t)$ is an added Gaussian noise with zero mean and unit variance, and σ is the noise intensity. When $\varepsilon = \varepsilon_x = \varepsilon_y$, then the systems are bidirectionally coupled, whereas $\varepsilon_x = 0$ corresponds to a unidirectional coupling configuration. When $\xi_x = \xi_y$, the Gaussian noise is common, otherwise it is independent. The function $f(x(t-\tau))$ is taken to be a symmetric piecewise linear function defined by

$$f(x) = A_{x,y}f^* - Bx. \quad (2a)$$

Here

$$f^* = \begin{cases} -x^* & x < -x^*, \\ x & -x^* \leqslant x \leqslant x^*, \\ x^* & x > x^*, \end{cases} \quad (2b)$$

where x^* is a controllable threshold value, $A_{x,y}$ and B are parameters. The parameter values are fixed in accordance with the values of the circuit elements [6]. The uncoupled system exhibits a chaotic attractor for the above values of the parameters as shown in Figs. 5 and 6 of Ref. [6].

III. NOISE-ENHANCED PS IN UNIDIRECTIONALLY COUPLED TIME-DELAY SYSTEMS

Now, we will demonstrate the results for unidirectional coupling. For the drive system $A_x = 5.2$ and for the response system $A_y = 5.0$, while B is fixed as $B = 3.5$. It is to be noted that the results presented in the entire paper remain invariant irrespective of the values of the parameters $A_{x,y}$, B, and b, which are chosen such that the individual systems exhibit chaotic behavior. The coupled system (1) is integrated using the Runge-Kutta fourth order integration scheme with step size 0.01 and the additive Gaussian noise is added at every integration step. Interacting chaotic dynamical systems are said to be in the phase synchronized state when there exists an entrainment between phases of the systems, while their amplitudes may remain chaotic and uncorrelated. In other words, PS exists when their respective frequencies and phases are locked [1,2]. The phase of a chaotic attractor can also be defined based on an appropriate Poincaré section, which the chaotic trajectory crosses once for each rotation; please refer to [1,2] for various other possible estimators (definition) of the phase. Each crossing of the orbit with the Poincaré section corresponds to an increment of 2π of the phase, and the phase in between two crosses is linearly interpolated as [1,2]

$$\Phi(t) = 2\pi k + 2\pi\frac{t - t_k}{t_{k+1} - t_k} \qquad (t_k < t < t_{k+1}), \quad (3)$$

where t_k is the time of kth crossing of the flow with the Poincaré section.

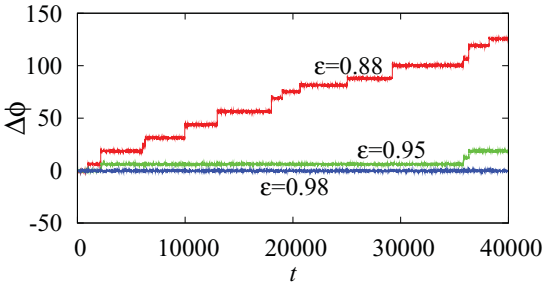

FIG. 1. (Color online) Phase difference for different values of the coupling strength ε, while the noise intensity $\sigma = 0.0$.

The Poincaré section is chosen at $x(t-\tau) = 0.8$ and $x(t) < 0.8$ on the attractor throughout the paper. The unidirectionally coupled, for $\varepsilon_x = 0$ and $\varepsilon = \varepsilon_y$, piecewise linear time-delay system exhibits PS for appropriate values of the coupling strength without noise $\sigma = 0$, which is indeed demonstrated in Fig. 1. In the absence of the coupling, both systems evolve independently with different frequencies due to the frequency mismatch $\omega_x \neq \omega_y$. For $\varepsilon = \varepsilon_y = 0.88$, the coupled systems are in their transition to the PS regime. Further increase in the coupling strength leads to increase in the duration of the phase synchronized epochs, finally resulting in the prefect PS. In particular, the coupled systems are at the onset of PS at $\varepsilon = 0.95$ and in prefect phase synchrony for $\varepsilon = 0.98$.

The mean frequency of the chaotic oscillations is defined as [1,2], $\Omega_{x,y} = \langle d\phi_{x,y}(t)/dt\rangle = \lim_{T\to\infty}\frac{1}{T}\int_0^T \dot{\phi}_{x,y}(t)dt$ and the $1:1$ PS between the coupled systems can also be characterized by the equality of their mean frequencies $\Omega_x = \Omega_y$. The mean frequency difference $\Delta\Omega = \Omega_y - \Omega_x$ as a function of $\varepsilon \in (0,1)$ for both a common and an independent noise with $\sigma = 0.006$, represented as connected open circles, are shown in Figs. 2(a) and 2(b), respectively. The solid line corresponds to the mean frequency difference in the absence of noise, $\sigma = 0$. Smaller values of the mean frequency difference $\Delta\Omega$, below the onset of exact PS at $\varepsilon_{PS} = 0.95$, for the connected circles compared to that of the solid line, clearly illustrate the phenomenon of noise-enhanced PS for both a common and an independent noise.

To demonstrate this phenomenon more clearly, we analyze the duration of PS epochs t_{epoch} as σ is increased. We choose $\varepsilon = 0.88$ well below ε_{PS} and $\xi_x = \xi_y$, that is, a common noise. The instantaneous phase difference $\Delta\phi$ for different σ is depicted in Fig. 2(c). In the absence of noise, $\sigma = 0$, the average phase difference displays several PS epochs, whereas the longest possible PS epochs are observed for $\sigma = 0.006$, which is indeed confirmed by the maximal value of the average duration of PS epochs $\langle t_{epoch}\rangle$ shown in Fig. 2(d) ($\langle t_{epoch}\rangle$ is estimated by averaging over ten different realizations, each of duration $t = 2\,000\,000$). Note that, as we have fixed the coupling strength well below the onset of perfect PS, we did not achieve perfect PS with noise. However, we have confirmed that if the coupling strength is chosen very close to the onset of perfect PS, noise can induce perfect PS in the coupled time-delay systems. Further increase in the noise intensity results in shortening of the duration of PS epochs as depicted for $\sigma = 0.016$ in Fig. 2(c) and lower values of the

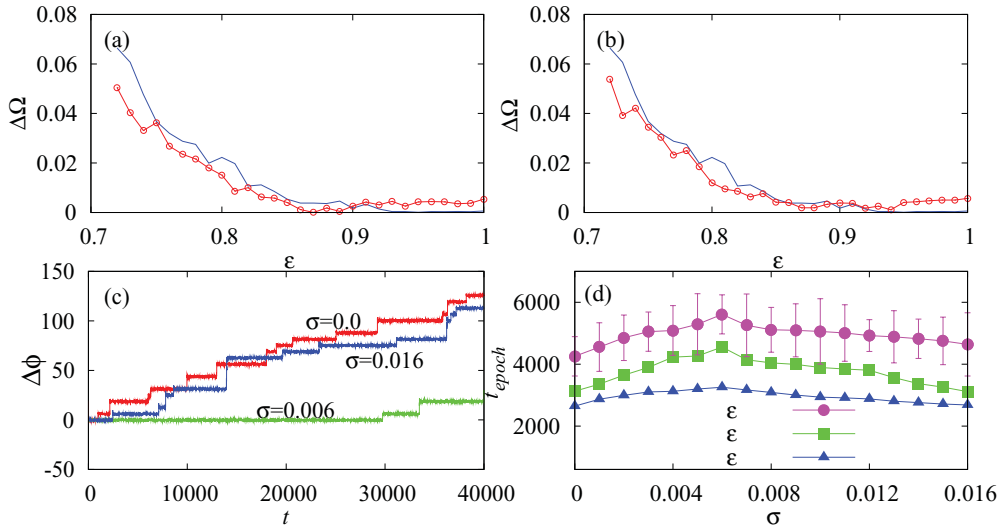

FIG. 2. (Color online) Frequency difference $\Delta\Omega$ vs coupling strength ε with a common noise (a) and with an independent noise (b) for unidirectional coupling. Solid line corresponds to $\sigma = 0$ and open circles to $\sigma = 0.006$. (c) Phase difference for different noise intensity σ and (d) average duration of PS epochs vs σ for different ε. The standard deviation is shown with error bars for $\varepsilon = 0.88$.

average duration of PS epochs $\langle t_{\text{epoch}} \rangle$ [see Fig. 2(d)]. Hence increasing σ from zero increases the average duration of PS epochs attaining a maximum for appropriate σ, attributing to noise-enhanced PS, and then $\langle t_{\text{epoch}} \rangle$ decreases for larger σ, like the resonance phenomenon due to the competing effects of the noise and the mutual locking of time scales of the coupled system, as we will discuss below. This behavior is also observed for the other values of the coupling strength, as illustrated in Fig. 2(d). We have also obtained qualitatively similar results for $\xi_x \neq \xi_y$, an independent noise.

Now, we investigate the return times T_k to a Poincaré section to understand the constructive role of noise in increasing the duration of PS epochs t_{epoch}. Periodic orbits are manifested by almost vanishing $\Delta X_k = |x_{t+k} - x_t|$ at the Poincaré section for every k returns with the corresponding return times T_k. PS is characterized by mutual phase locking of unstable

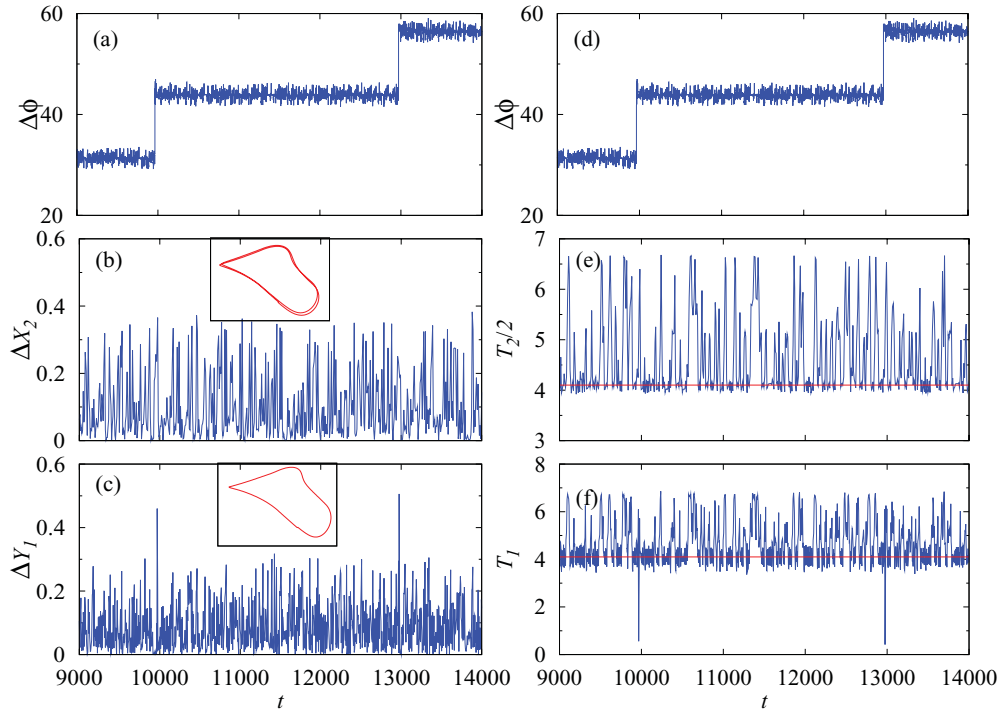

FIG. 3. (Color online) (a) Phase slips induced by unlocked UPOs are illustrated in (a) and (d). Difference between x and y variables, ΔX_2 and ΔY_1, to the Poincaré section is shown in (b) and (c), respectively, with the insets illustrating period-2 and period-1 unlocked UPOs around $t \approx 9950$ and their corresponding return times T_2 and T_1 in (e) and (f), respectively.

periodic orbits (UPOs) of the coupled chaotic systems and the phase slips are manifested by a few pairs of unlocked UPOs of the coupled system similar to periodically driven chaotic oscillators [1,2,13,16]. Noise is capable of preventing the systems from following unlocked UPOs for a long time and also forcing the systems to follow them for a long time resulting in both short and long return times, which do not happen in noise-free systems [13]. This is illustrated in Fig. 3 for $\varepsilon = 0.88$ and for the small noise intensity $\sigma = 0.002$. A phase synchronized epoch along with the accompanying phase slips at both ends is depicted in Figs. 3(a) and 3(d). Note that both these figures are the same and are shown here to compare the region of phase slips with the other figures. The difference between the same variables ΔX_2 and ΔY_1 for every second and first returns, with return times T_2 and T_1, to the Poincaré section is shown in Figs. 3(b) and 3(c), respectively, along with their corresponding period-2 and period-1 UPOs in the insets. It is to be noted that the large fluctuation in the difference ΔX_2 and ΔY_1 is due to the oscillations with different (multiple) time scale returns to the Poincaré section at different instants in contrast to the mutually coupled systems (see below). The phase slip at $t \approx 9950$ is indeed caused by these pairs of unlocked UPOs, which is followed by the system for sufficiently long time for a phase slip to occur. Nevertheless, one can also find other pairs of unlocked UPOs at the phase slip while the majority of the UPOs of the coupled systems are mutually locked. Those pairs with small and large return times [see Fig. 3(f)], corresponding to a large mismatch in their time scales, require a large value of coupling strength for a fixed noise intensity to become locked. On the contrary, a large value of the noise intensity, less than a certain threshold for a fixed coupling strength, can also change their time scales to become locked, consequently increasing the duration of PS epochs t_{epoch} resulting in noise-enhanced PS as shown in Fig. 2.

Multiple time scales of the individual system are clearly identified from their return times [Figs. 3(e) and 3(f)]. The principle time scale, around which a majority of the return times are fluctuating, is indicated by a horizontal line at 4.3, while the other two pronounced time scales are seen at 5.3 and 6.6. It is to be noted that the time scales of the drive system remain unaffected [see Fig. 3(e)], while most of the time scales of the response system become entrained to that of the drive system except those return times with a large difference in the time scales of unlocked UPOs manifesting phase slips [compare Figs. 3(d) and 3(f)].

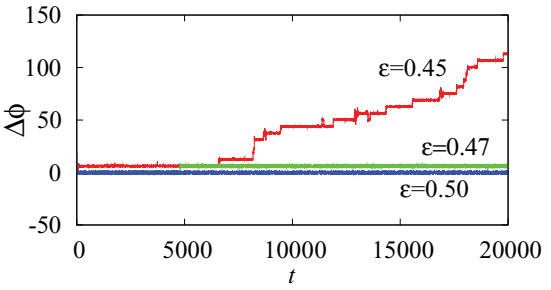

FIG. 4. (Color online) Phase difference for different values of the coupling strength ε, while the noise intensity $\sigma = 0.0$, for the bidirectionally coupled piecewise linear time-delay systems.

IV. NOISE-ENHANCED PS IN BIDIRECTIONALLY COUPLED TIME-DELAY SYSTEMS

In the following, we will demonstrate the phenomenon of noise-enhanced PS in bidirectionally coupled time-delay systems where both subsystems adjust their time scales of oscillation to their principle time scale in achieving PS. Now, we fix the same parameters as above except for $A_x = A_y = 5.2$, that is, parameter mismatch only in the frequencies. The instantaneous phase difference of the bidirectionally coupled piecewise linear time-delay system is shown in Fig. 4 for different ε but without noise $\sigma = 0.0$. Because of the frequency mismatch, both systems evolve independently for $\varepsilon = 0.0$.

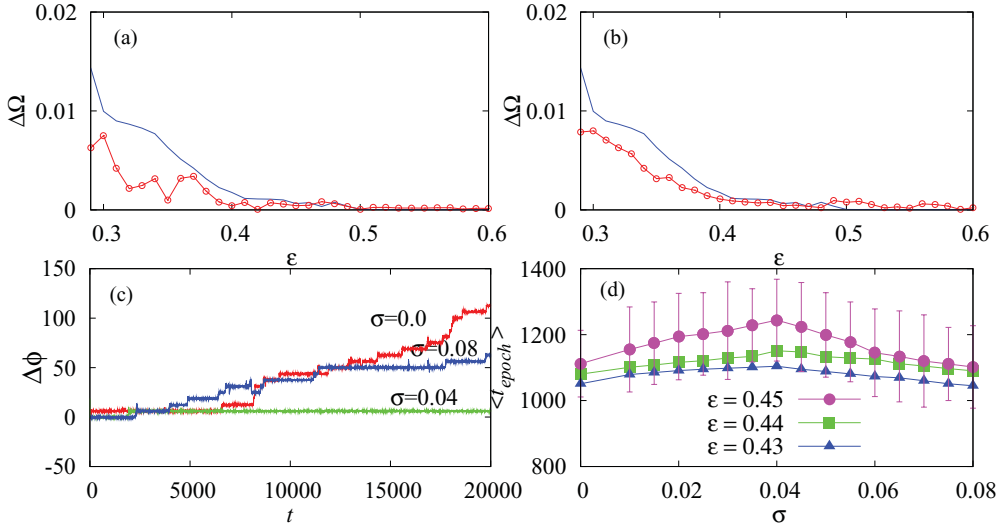

FIG. 5. (Color online) Bidirectional coupling: Frequency difference $\Delta\Omega$ vs coupling strength ε with a common noise (a) and with an independent noise (b). Solid line corresponds to $\sigma = 0$ and open circles to $\sigma = 0.04$. (c) Phase difference for different noise intensity σ and (d) average duration of PS epochs vs σ for different ε. The standard deviation is shown with error bars for $\varepsilon = 0.45$.

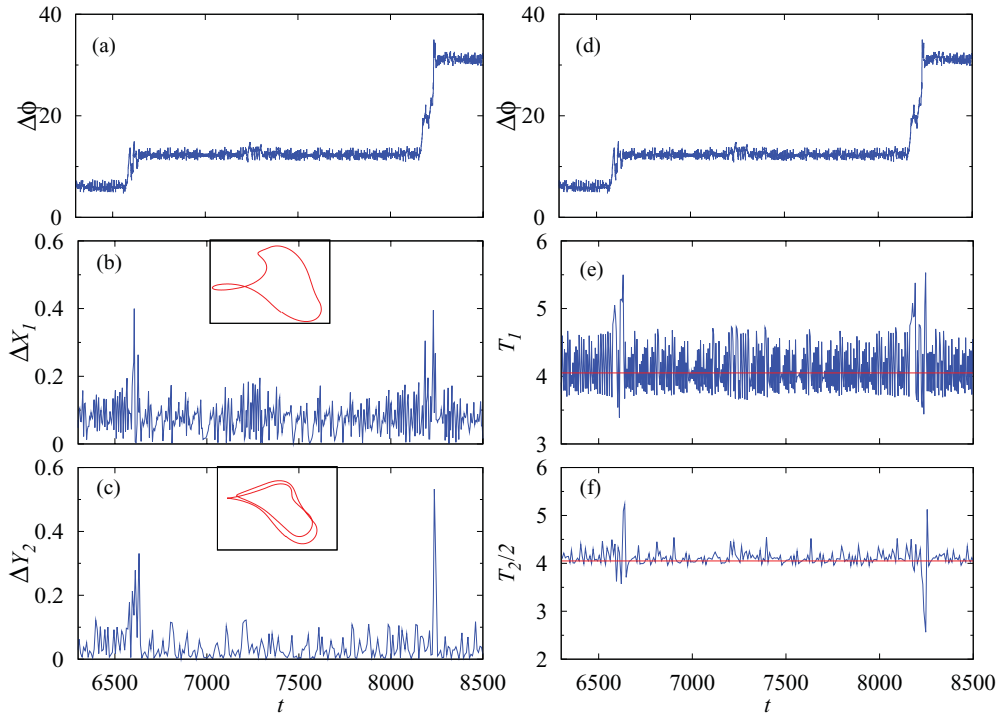

FIG. 6. (Color online) (a) Phase slips induced by unlocked UPOs are illustrated in (a) and (d). Difference between x and y variables, ΔX_1 and ΔY_2, on the Poincaré section is shown in (b) and (c), respectively, with the insets illustrating period-2 and period-1 unlocked UPOs around $t \approx 6600$ and their corresponding return times T_1 and T_2 in (e) and (f), respectively.

The coupled systems are in their transition to PS for both $\varepsilon = 0.45$ and 0.47, while they are in perfect PS for $\varepsilon = 0.5$. The average frequency difference $\Delta\Omega$ is depicted in Figs. 5(a) and 5(b) in the presence of a common and an independent noise, respectively, with $\sigma = 0.04$, indicated by connected open circles. The solid line corresponds to $\Delta\Omega$ without any noise. $\Delta\Omega$ acquire small values in the presence of noise rather than without noise in almost the entire range of the coupling strength below $\varepsilon_{\rm PS} = 0.5$, which clearly indicates the phenomenon of noise-enhanced PS in bidirectionally coupled systems. The phase difference $\Delta\phi$ for different values of the noise intensity σ with a common Gaussian noise and $\varepsilon = 0.45$ are shown in Fig. 5(c). The average duration of PS epochs $\langle t_{\rm epoch}\rangle$ for three different values of the coupling strength ε is illustrated in Fig. 5(d). From these figures, it is observed that the duration of PS epochs increases with noise intensity and reaches a maximum for an optimal value of the noise intensity with further increase in it resulting in decreasing in the value of $\langle t_{\rm epoch}\rangle$, similar to the phenomenon of resonance due to the competition between the noise and the mutual locking of UPOs. Similar results are obtained for other analyzed values of the coupling strength and for an independent noise.

A phase synchronized epoch with its accompanying phase slips is illustrated in Figs. 6(a) and 6(d) for $\varepsilon = 0.45$ and $\sigma = 0.01$. The difference between the same variables, ΔX_1 and ΔY_2, at every first and second return to the Poincaré section are shown in Figs. 6(b) and 6(c), respectively. The phase slip around $t \approx 6600$ is occurred between the unlocked period-2 and period-1 UPOs depicted in the insets. One can also find other pairs of unlocked UPOs at this phase slip. Being a bidirectionally coupled system, the subsystems adjust their time scales to their principle time scale, indicated by the horizontal line at 4.05, around which the majority of the return times fluctuate, attributing to the majority of locked UPOs. The small and large return times in both subsystems at $t \approx 6600$ and $t \approx 8250$ in Figs. 6(e) and 6(f) is due to the large difference in the time scales of the pair of unlocked UPOs. As discussed for the unidirectional coupling, it requires a large coupling strength or a large noise less than a threshold value to induce changes in their time scales such that the UPOs now become locked. The latter is indeed demonstrated in Fig. 5(c) for the noise intensity $\sigma = 0.04$, and in Fig. 5(d) illustrating the increase in the duration of PS epochs resulting in noise-enhanced PS for fixed values of the coupling strength.

V. SUMMARY AND CONCLUSION

In summary, we have demonstrated the phenomenon of noise-enhanced PS in both unidirectionally and bidirectionally coupled time-delay systems. It is to be noted that the time scales of the drive system remain unaffected, while most of the time scales of the response system are entrained to that of the drive system in unidirectionally coupled time-delay systems, whereas both systems adjust their rhythms to their principle time scale for mutual coupling. In particular, the return time clearly indicates the multiple time scales of the delay system. Several rather complicated techniques, such as permutation information theory [17], principle component analysis [18], etc., have been developed to identify the time scales, whereas our result shows that this could be clearly seen from the return times. Entrainment of the oscillations to the principle time scale in mutually coupled systems despite

the presence of intrinsic multiple time scales could shed more light on our understanding of information processing in neural networks where the connections naturally involves delay and exhibit multiple time scale. Further, synchronizing to a particular time scale, correspondingly to a specific frequency, for instance α and β waves in the brain [19], could enrich our knowledge on synchronization and its control of several pathological disorders, in chaotic semiconductor lasers [17], etc. Experimental confirmation of the above results are in progress using electronic circuits [6]. We have confirmed that the reported phenomenon does change for a range of values of the parameters in the chaotic regime and hence our results remain robust against the changes in the parameters.

ACKNOWLEDGMENTS

D.V.S and J.K. acknowledge support from EU under Project No. 240763 PHOCUS(FP7-ICT-2009-C).

[1] A. S. Pikovsky, M. G. Rosenblum, and J. Kurths, *Synchronization—A Unified Approach to Nonlinear Science* (Cambridge University Press, Cambridge, England, 2001).

[2] S. Boccaletti, J. Kurths, G. Osipov, D. L. Valladares, and C. S. Zhou, Phys. Rep. **366**, 1 (2002).

[3] A. Arenas, A. Díaz-Guilera, J. Kurths, Y. Moreno, and C. S. Zhou, Phys. Rep. **469**, 93 (2008).

[4] M. Lakshmanan and D. V. Senthilkumar, *Dynamics of Nonlinear Time-delay Systems* (Springer, Berlin, 2011).

[5] V. Flunkert, S. Yanchuk, T. Dahms, and E. Schöll, Phys. Rev. Lett. **105**, 254101 (2010); M. Dhamala, V. K. Jirsa, and M. Ding, *ibid.* **92**, 074104 (2004); C. Masoller and A. C. Marti, *ibid.* **94**, 134102 (2005); F. M. Atay, J. Jost, and A. Wende, *ibid.* **92**, 144101 (2004); A. Englert, S. Heiligenthal, W. Kinzel, and I. Kanter, Phys. Rev. E **83**, 046222 (2011).

[6] D. V. Senthilkumar, K. Srinivasan, K. Murali, M. Lakshmanan, and J. Kurths, Phys. Rev. E **82**, 065201(R) (2010).

[7] D. V. Senthilkumar, M. Lakshmanan, and J. Kurths, Phys. Rev. E **74**, 035205(R) (2006); R. Suresh, D. V. Senthilkumar, M. Lakshmanan, and J. Kurths, *ibid.* **82**, 016215 (2010).

[8] G. C. Sethia, A. Sen, and F. M. Atay, Phys. Rev. Lett. **100**, 144102 (2008); A. Prasad, J. Kurths, S. K. Dana, and R. Ramaswamy, Phys. Rev. E **74**, 035204(R) (2006).

[9] F. Varela, J. P. Lachaux, E. Rodriguez, and J. Martinerie, Neurosci. (Nat. Rev.) **2**, 229 (2001).

[10] J. Fell and N. Axmacher, Neurosci. (Nat. Rev.) **12**, 105 (2011).

[11] G. Deco, V. Jirsa, A. R. McIntosch, O. Sporns, and R. Kötter, Proc. Natl. Acad. Sci. USA **106**, 10302 (2009).

[12] P. Ashwin, J. Buescu, and I. Stewart, Phys. Lett. A **193**, 126 (1994).

[13] C. Zhou, J. Kurths, I. Z. Kiss, and J. L. Hudson, Phys. Rev. Lett. **89**, 014101 (2002); C. Zhou and J. Kurths, *ibid.* **88**, 230602 (2002); K. H. Nagai and H. Kori, Phys. Rev. E **81**, 065202(R) (2010).

[14] V. S. Anishchenko, V. Astakhov, A. Neiman, T. Vadivasov, and L. Schimansky-Geier, *Nonlinear Dynamics of Chaotic and Stochastic Systems* (Springer, Berlin, 2002); W. Horsthemke, and R. Lefever, *Noise-Induced Transitions: Theory and Applications in Physics, Chemistry and Biology* (Springer, Berlin, 1984).

[15] H. A. Shadlow, Neurphysiol. **54**, 1346 (1985); F. Aboitiz, A. B. Scheibel, R. S. Fisher, and E. Zaidel, Brain Res. **598**, 143 (1992).

[16] A. Pikovsky, G. Osipov, M. Rosenblum, M. Zaks, and J. Kurths, Phys. Rev. Lett. **79**, 47 (1997); M. A. Zaks, E. H. Park, M. G. Rosenblum, and J. Kurths, *ibid.* **82**, 4228 (1999).

[17] M. C. Soriano, L. Zunino, O. A. Rosso, I. Fischer, and C. R. Mirasso, IEEE J. Quantum Electron. **47**, 252 (2011).

[18] I. T. Jolliffe, *Principal Component Analysis* (Springer, New York, 2002).

[19] R. R. Llinas, A. A. Grace, and Y. Yarom, Proc. Natl. Acad. Sci. USA **88**, 897 (1991).